Diamond-like carbon thin film deposition using low-energy ion beams

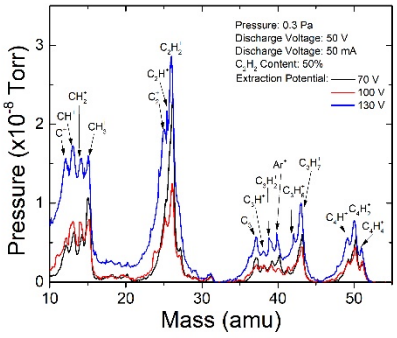

Figure 1. Mass spectra of Ar:C_2H_2 plasma at 50% C_2H_2 content and various φ_{ext}.

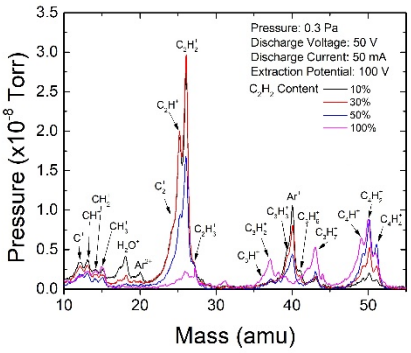

Figure 2. Mass spectra of Ar:C_2H_2 plasma at φ_{ext} = 100 V and various C_2H_2 content.

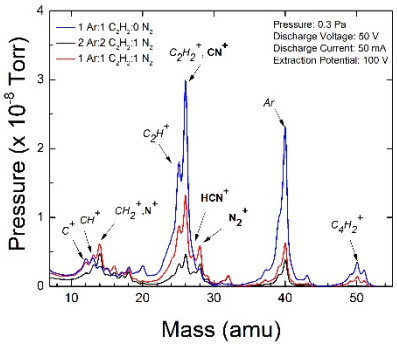

Figure 3. Mass spectra of the Ar:C_2H_2:N_2 plasma at φ_{ext} = 100 V and various N_2 content.

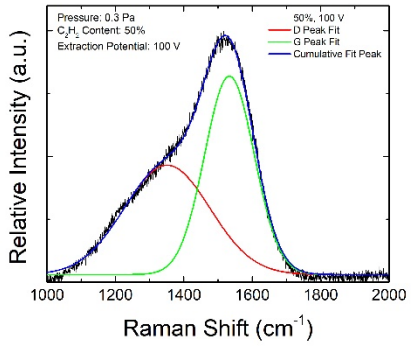

Figure 4. Sample deconvolution of DLC Raman spectrum at visible light irradiation (532 nm). D and G fits and peaks are labeled respectively

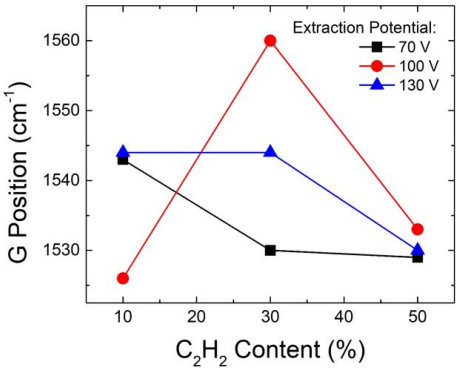

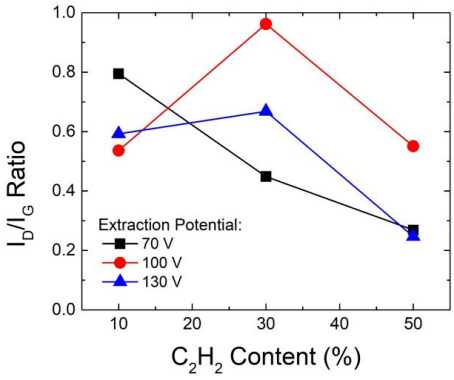

Figure 5. G positions and I_D/I_G ratios calculated from the deconvoluted D and G peaks acquired from the Raman spectra of films illuminated using visible light.

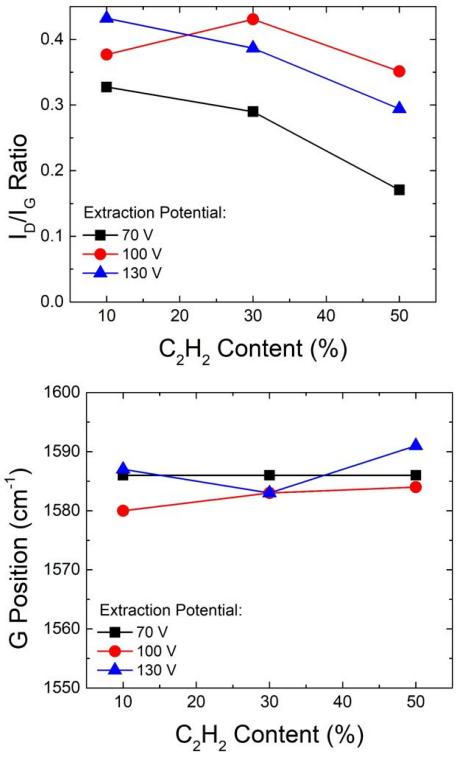

Figure 6. G positions and I_D/I_G ratios calculated from the deconvoluted D and G peaks acquired from the Raman spectra of films illuminated using UV light.

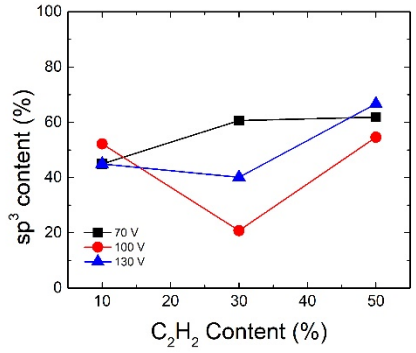

Figure 7. Calculated sp^3 fraction using the model (Eq. 2.5) derived by Cui et al. (2010) from the I_D/I_G ratios and G positions of deconvoluted D and G peaks obtained from visible and UV Raman spectroscopy.

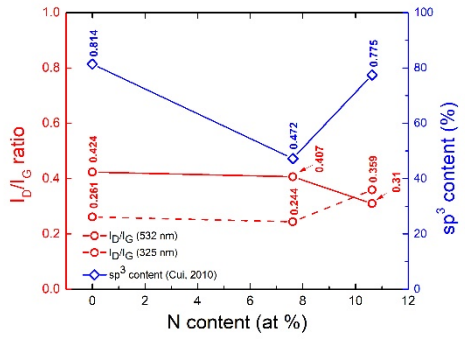

Figure 8. The variation of the G position and I_D/I_G from the obtained D and G peak deconvolution for N-doped and undoped samples.

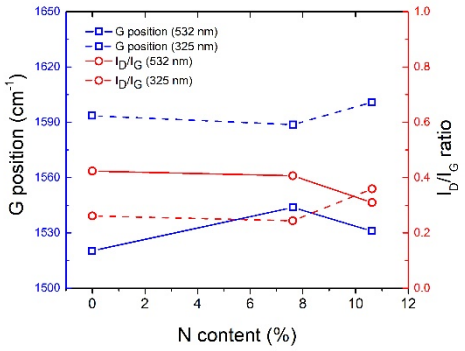

Figure 9. The variation of sp^3 content obtained empirically by (Cui et al., 2010) for N-doped and undoped samples.

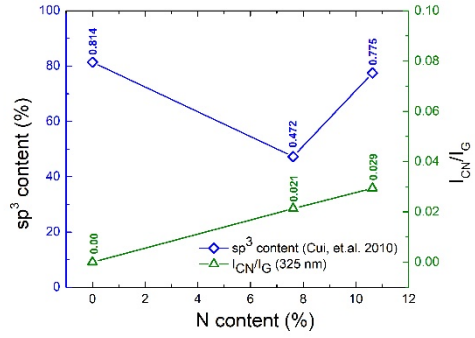

Figure 9. The variation of the I_{CN} /I_G and sp^3 content for N-doped samples